organic compounds

Metabolic pathways of dithiocarbamates from laboratory powder diffraction data

Vladimir V. Chernyshev,[a]* Ksenia A. Paseshnichenko,[a] Vadim A. Makarov,[b] Eduard J. Sonneveld[c] and Hendrik Schenk[c]

[a]Chemistry Department, Moscow State University, 119899 Moscow, Russia, [b]State Scientific Centre 'NIOPIK', Department of Medicinal Chemistry, B. Sadovaya str. 1-4, 103787 Moscow, Russia, and [c]Laboratory of Crystallography, University of Amsterdam, Nieuwe Achtergracht 166, Amsterdam, 1018 WV, The Netherlands
Correspondence e-mail: cher@biocryst.phys.msu.su

In order to correlate the reactivity and molecular structures of dithiocarbamates, the crystal structures of 6-dimethyl-amino-5-nitropyrimidin-4-yl N,N-diethyldithiocarbamate, $C_{11}H_{17}N_5O_2S_2$, (Ia), and 6-methylamino-5-nitropyrimidin-4-yl N,N-diethyldithiocarbamate, $C_{10}H_{15}N_5O_2S_2$, (Ib), and of the product of thermolysis of (Ib), namely 4-diethylamino-6-methylamino-5-nitropyrimidinium chloride monohydrate, $C_9H_{16}N_5O_2{}^+\cdot Cl^-\cdot H_2O$, (II), have been determined from X-ray laboratory powder diffraction data. Conformational preferences in (Ia) and (Ib) were studied on the density functional theory (DFT) level. Deviation of the reaction centre of the molecule from planarity and breakage of the secondary $S\cdots O$ contact cause switching between two alternative pathways of thermolysis.

Comment

Dithiocarbamoyl derivatives of diverse heterocycles demonstrate a broad range of physiological activity; antifilarial (Gallay & Schweizer, 1980), antiviral (Bernstein et al., 1993) and antifungal agents (Itoh & Okonogi, 1995), and oncolytic (Lerchen et al., 1996) and lipoprotein disorder drugs (Tokuhisa et al., 1998) are known among this group of compounds. Therefore, the question of the possible metabolic pathways of such compounds is currently a very hot topic in medicinal chemistry and the systematic study of their reactivity can clarify this problem. Three such compounds, (Ia), (Ib) and (II), are discussed here.

It has been demonstrated that the thermolysis of dithiocarbamoyl derivatives of pyridines and pyrimidines containing a nitro group ortho to the dithiocarbamoyl moiety (Ia) can result in the formation of disulfide compounds with elimination of the nitro group [(III); Rasheed & Warkentin, 1977; Makarov et al., 1994). Recently, an alternative thermolysis pathway involving the elimination of carbon disulfide has been found [(Ib)→(IV); Makarov et al., 2001]. The different reactivity of (Ia) and (Ib) can be interpreted, in principle, in terms of the differences in their molecular structures, which are illustrated in Table 1 and Fig. 1; the twist of the nitro group out of the plane of the pyrimidine ring in (Ia) should lower its
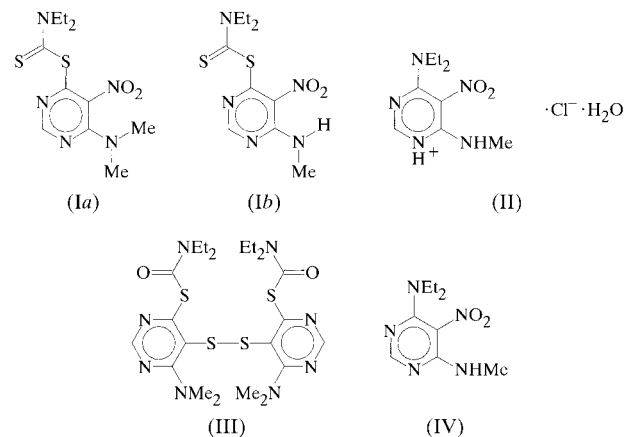
affinity for nucleophilic substitution compared with (Ib). Besides this, the twist of the nitro group in (Ia) breaks the secondary $S\cdots O$ contact, which is present in (Ib). Short intramolecular $S\cdots O$ contacts arise from the σ-interaction between the non-bonding orbital of the O atom and the p and d orbitals of the S atom, and this interaction affects the spectral and chemical properties of the corresponding compounds (Cohen-Addad et al., 1984).
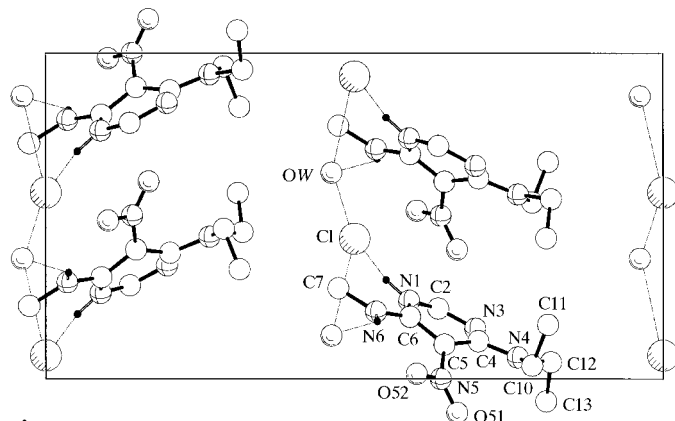
The results of the density functional theory (DFT) geometrical optimization of (Ib) decribed below compare
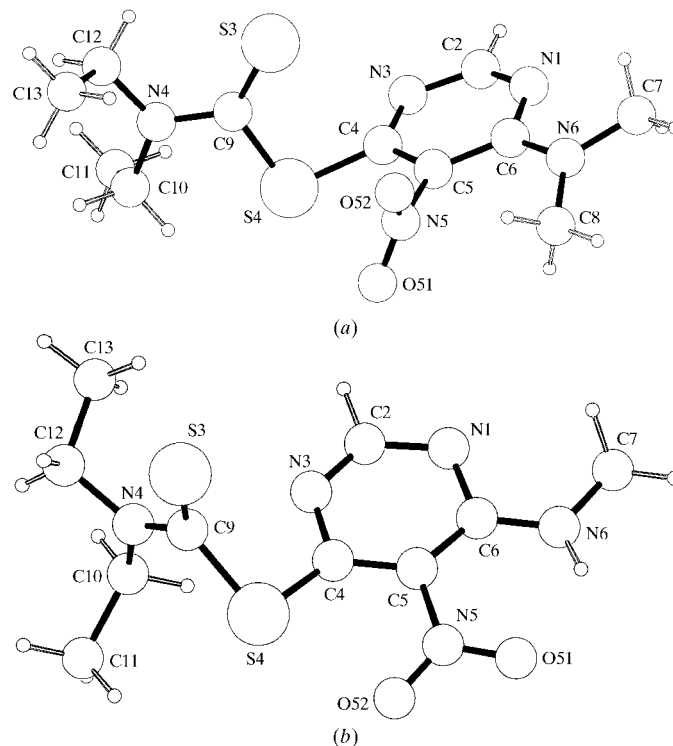
Figure 1
The molecular structures of (a) (Ia) and (b) (Ib) with the atomic numbering.

rather well with the crystallographic data. Therefore, only minor changes in the molecular geometry of (I*b*) are expected upon transfer from the crystal to solution. The secondary S···O contact also maintains the orientation of the dithiocarbamate group with respect to the C4—S4 bond; according to the DFT data, the decrease of the C5—C4—S4—C9 torsion angle from 169 to 110° (close to the observed value of 103°) requires 26 kJ mol^{-1}. The orienting effect of the S···O contacts is also confirmed by analysis of the data retrieved from the Cambridge Structural Database (CSD; Allen & Kennard, 1993) on compounds with the S*R* group situated *ortho* to the nitro group; in all 98 structures where the twist angle of the nitro group is less than 30°, the *R* moiety lies close to the ring plane and the NO$_2$ and S*R* groups behave like engaged gears. However, if the nitro group is twisted out of the ring plane, the *R*—S—C—C torsion angles fall in the range 50–175° (14 structures).

In contrast with (I*b*), the geometrical optimization of (I*a*) leads to a structure that is significantly different from that observed, not only in terms of geometry, but also in terms of energy (the optimization started from the X-ray molecular geometry). Recently, two energy minima have been found for 2-nitrobenzenethiolates on the *AM*1 level (Dewar *et al.*, 1985), the main one corresponding to the in-plane orientation of the nitro group and the second (local) one corresponding to the broken S···O contact (Low *et al.*, 2000). In compounds (I*a*) and (I*b*), the DFT study did not reveal the second energy minimum. This distinction is probably due to the known deficiences in the sulfur parametrization inherent in the *AM*1 Hamiltonian. In particular, *AM*1 overestimates the positive charge on the S atoms, as compared with the *ab initio* results (Storer *et al.*, 1995). The heat of formation obtained in the geometrical optimization, with the C5—C4—S4—C9 torsion angle constrained at its experimental value, is 16 kJ mol^{-1} higher than that for the fully optimized geometry. Thus, there are good reasons to believe that (I*a*) flattens upon transfer from a crystal to solution and this is the probable reason why the thermolysis of (I*a*) proceeds faster in the solid state than in xylene solution at the same temperature (Makarov *et al.*, 1994). On the other hand, this means that even moderate deviation of the reaction centre of the molecule from planarity is enough to switch between two thermolysis pathways. Short

intermolecular contacts are absent from the structures of (I*a*) and (I*b*).

The thermolysis product of (I*b*) was isolated as the monohydrochloride salt, (II). The protonation site was unambiguously determined from analysis of the cation–anion contacts: N1···Cl 3.07 (1) Å and N1—H1···Cl 152 (4)°. However, the DFT and *AM*1 calculations predict that the protonation sites at N1 and N3 are equivalent to within 4 kJ mol^{-1}; thus, this compound should exist in solution as a tautomeric mixture. The hydrogen-bonding motif in (II) is shown in Fig. 2. The OW···Cl distances are 3.14 (1) and 3.19 (1) Å, and the Cl···OW···Cl angle is 117 (1)°. Besides this, the water molecule forms a weak hydrogen bond to the methylamino group: OW···H6^i 2.22 (5) Å [symmetry code: (i) $x - \frac{1}{2}, \frac{1}{2} - y, z$].
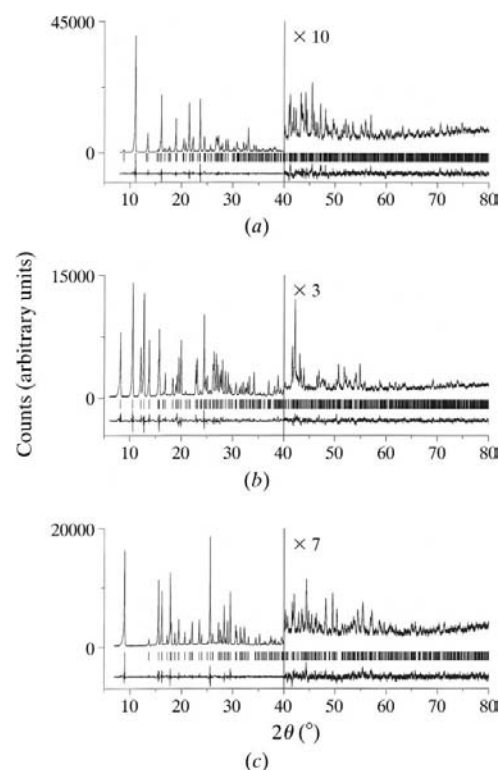
Figure 3
The Rietveld plots, showing the observed and difference profiles, for (*a*) (I*a*), (*b*) (I*b*) and (*c*) (II). The reflection positions are shown above the difference profile.

Experimental

Compounds (I*a*), (I*b*) and (II) were prepared in polycrystalline form according to the procedure of Makarov *et al.* (2001).

Compound (I*a*)

Crystal data

C$_{11}$H$_{17}$N$_5$O$_2$S$_2$	Cu *K*α radiation
$M_r = 315.42$	λ = 1.54059 Å
Orthorhombic, *Pbca*	μ = 3.228 mm^{-1}
$a = 20.013$ (6) Å	$T = 295$ (2) K
$b = 13.456$ (3) Å	Specimen shape: flat sheet
$c = 11.424$ (3) Å	7 × 7 × 1.5 mm
$V = 3076$ (1) Å^3	Particle morphology: no specific
$Z = 8$	habit, intense yellow
$D_x = 1.362$ Mg m^{-3}	

Figure 2
A packing diagram for (II) with the atomic numbering.

organic compounds

Data collection

Enraf–Nonius diffractometer with Guinier Johannson camera FR 552
Specimen mounting: pressed as a thin layer in the specimen holder of the camera
Specimen mounted in transmission mode

$T = 295 (2)$ K
$h = 0 \rightarrow 16$
$k = 0 \rightarrow 11$
$l = 0 \rightarrow 9$
$2\theta_{min} = 4.03$, $2\theta_{max} = 80.0°$
Increment in $2\theta = 0.01°$

Refinement

Refinement on I_{net}
$R_p = 0.073$
$R_{wp} = 0.098$
$R_{exp} = 0.030$
$S = 3.22$
$2\theta_{min} = 8$, $2\theta_{max} = 80°$
Increment in $2\theta = 0.01°$
Wavelength of incident radiation: 1.54059 Å
Excluded region(s): 4.03–7.99

Profile function: split-type pseudo-Voigt
155 parameters
H-atom parameters constrained
Weighting scheme based on measured s.u.'s
$(\Delta/\sigma)_{max} = 0.05$
$\Delta\rho_{max} = 0.5$ e Å^{-3}
$\Delta\rho_{min} = -0.5$ e Å^{-3}
Preferred orientation correction: March–Dollase (Dollase, 1986)

Compound (Ib)

Crystal data

$C_{10}H_{15}N_5O_2S_2$
$M_r = 301.39$
Monoclinic, $P2_1/c$
$a = 7.354 (3)$ Å
$b = 9.098 (4)$ Å
$c = 21.738 (8)$ Å
$\beta = 97.33 (2)°$
$V = 1443 (1)$ Å^3
$Z = 4$

$D_x = 1.388$ Mg m^{-3}
Cu $K\alpha$ radiation
$\lambda = 1.54059$ Å
$\mu = 3.417$ mm^{-1}
$T = 295 (2)$ K
Specimen shape: flat sheet
$7 \times 7 \times 1.5$ mm
Particle morphology: parallele-piped, dark yellow

Data collection

Enraf–Nonius diffractometer with Guinier Johannson camera FR 552
Specimen mounting: pressed as a thin layer in the specimen holder of the camera
Specimen mounted in transmission mode

$T = 295 (2)$ K
$h = 0 \rightarrow 6$
$k = 0 \rightarrow 7$
$l = -18 \rightarrow 17$
$2\theta_{min} = 4.05$, $2\theta_{max} = 80.0°$
Increment in $2\theta = 0.01°$

Refinement

Refinement on I_{net}
$R_p = 0.075$
$R_{wp} = 0.102$
$R_{exp} = 0.035$
$S = 2.94$
$2\theta_{min} = 6$, $2\theta_{max} = 80°$
Increment in $2\theta = 0.01°$
Wavelength of incident radiation: 1.54059 Å
Excluded region(s): 4.05–5.99

Profile function: split-type pseudo-Voigt
142 parameters
H-atom parameters constrained
Weighting scheme based on measured s.u.'s
$(\Delta/\sigma)_{max} = 0.05$
$\Delta\rho_{max} = 0.7$ e Å^{-3}
$\Delta\rho_{min} = -0.4$ e Å^{-3}
Preferred orientation correction: March–Dollase (Dollase, 1986)

Compound (II)

Crystal data

$C_9H_{16}N_5O_2{}^+\cdot Cl^-\cdot H_2O$
$M_r = 279.73$
Orthorhombic, $Pna2_1$
$a = 10.271 (3)$ Å
$b = 6.8360 (2)$ Å
$c = 19.642 (2)$ Å
$V = 1379.1 (6)$ Å^3
$Z = 4$
$D_x = 1.347$ Mg m^{-3}

Cu $K\alpha$ radiation
$\lambda = 1.54059$ Å
$\mu = 2.563$ mm^{-1}
$T = 295 (2)$ K
Specimen shape: flat sheet
$7 \times 7 \times 1.5$ mm
Particle morphology: needle, pale yellow

Data collection

Enraf–Nonius diffractometer with Guinier Johannson camera FR 552
Specimen mounting: pressed as a thin layer in the specimen holder of the camera
Specimen mounted in transmission mode

$T = 295 (2)$ K
$h = 0 \rightarrow 8$
$k = 0 \rightarrow 5$
$l = 0 \rightarrow 16$
$2\theta_{min} = 4.02$, $2\theta_{max} = 80.0°$
Increment in $2\theta = 0.01°$

Refinement

Refinement on I_{net}
$R_p = 0.080$
$R_{wp} = 0.105$
$R_{exp} = 0.037$
$S = 2.86$
$2\theta_{min} = 7$, $2\theta_{max} = 80°$
Increment in $2\theta = 0.01°$
Wavelength of incident radiation: 1.54059 Å
Excluded region(s): 4.02–6.99

Profile function: split-type pseudo-Voigt
141 parameters
H-atom parameters constrained
Weighting scheme based on measured s.u.'s
$(\Delta/\sigma)_{max} = 0.05$
$\Delta\rho_{max} = 0.6$ e Å^{-3}
$\Delta\rho_{min} = -0.5$ e Å^{-3}
Preferred orientation correction: March–Dollase (Dollase, 1986)

Table 1
Experimental and DFT-calculated geometric parameters (Å,°) defining the conformations of (Ia) and (Ib).

	X-ray	DFT
(Ia)		
C5—C4—S4—C9	103.9 (5)	164
C4—C5—N5—O51	62.6 (7)	34
C5—C6—N6—C8	12 (1)	19
N1—C6—N6—C7	8.0 (9)	14
S3—C9—S4—C4	−17.1 (5)	−103
S4···O51	2.964 (7)	2.687
(Ib)		
C5—C4—S4—C9	148.9 (7)	169
C4—C5—N5—O52	14.3 (9)	2
C5—C6—N6—C7	175.5 (6)	180
S3—C9—S4—C4	−93.8 (5)	−105
S4···O52	2.636 (7)	2.591

During the exposures, each specimen was spun in its plane to improve particle statistics. The unit-cell dimensions were determined from the Guinier photographs using the indexing program *ITO* (Visser, 1969) and refined with the program *LSPAID* (Visser, 1986) to $M_{20} = 25$ and $F_{30} = 69$ (0.010, 41) for (Ia), $M_{20} = 49$ and $F_{30} = 121$ (0.006, 40) for (Ib), and $M_{20} = 47$ and $F_{30} = 99$ (0.009, 35) for (II), using the first 50 peak positions. The space groups *Pbca*, $P2_1/c$ and $Pna2_1$ were chosen on the basis of systematic extinction rules for (Ia), (Ib) and (II), respectively. Intensities for the structure determination and refinement were measured from the Guinier photographs in 0.01° steps using a Johannson LS18 line scanner. The structures of (Ia) and (Ib) were solved by the grid search procedure (Chernyshev & Schenk, 1998). Preliminary information about the possible structures of (Ia) and (Ib) was obtained from IR and NMR spectroscopy and mass spectrometry. The approximate models of the molecules were built up with the program *MOPAC*6.0 (Stewart, 1990). In (II), the position of the Cl$^-$ anion was found first from the Patterson map. Subsequently, the cation was located in the unit cell using the grid search procedure. Finally, the position of the O atom from the solvent water, without H atoms, was also found by the grid search procedure.

The conformations of the molecules of (I*a*) and (I*b*) and of the cation of (II) changed significantly during the subsequent bond-restrained Rietveld refinements, leading to the correct crystal structures. The strength of the restraints was a function of interatomic separation and for intramolecular bond lengths corresponds to an r.m.s. deviation of 0.03 Å. The diffraction profiles and the differences between the measured and calculated profiles are shown in Fig. 3. H atoms were placed in geometrically calculated positions and allowed to refine using bond restraints, with a common isotropic displacement parameter U_{iso} fixed to 0.05 Å^2. The March–Dollase texture formalism (Dollase, 1986), with [010], [100] and [001] as the directions of preferred orientation, was applied for (I*a*), (I*b*) and (II), respectively. The texture parameter *r* refined to 0.86 (1), 1.08 (1) and 1.14 (1) for (I*a*), (I*b*) and (II), respectively. The DFT calculations were performed using the program provided by Dr D. N. Laikov (Laikov, 1997) employing the BLYP (Becke–Lee–Yang–Parr) exchange-correlation functional (Becke, 1988; Lee *et al.*, 1988). For the representation of the Kohn–Sham one-electron wave functions, the sets of contracted Gaussian-type functions were used; the contracted patterns were {311/1} for H, {611111/411/11} for C, N and O, and {6111111111/5111111/11} for S. For the expansion of the electron density, the uncontracted basis sets (5*s*1*p*) for H, (10*s*3*p*3*d*1*f*) for C, N and O, and (14*s*7*p*7*d*1*f*1*g*) for S were employed.

For all compounds, data collection: Johannson LS18 line scanner data collection program; cell refinement: *LSPAID* (Visser, 1986); data reduction: *PROFIT for Windows* (Philips, 1996); program(s) used to solve structure: *MRIA* (Zlokazov & Chernyshev, 1992); program(s) used to refine structure: *MRIA*; molecular graphics: *PLUTON* (Spek, 1992); software used to prepare material for publication: *MRIA*, *SHELXL*93 (Sheldrick, 1993) and *PARST* (Nardelli, 1983).

References

Allen, F. H. & Kennard, O. (1993). *Chem. Des. Autom. News*, **8**, 1, 31–37.
Becke, A. D. (1988). *Phys. Rev. A*, **38**, 3098–3100.
Bernstein, D. I., Rheins, L. A., Beitman, R. & Delehanty, J. (1993). *Antivir. Res.* **20**, Suppl. 1, Abstr. 171.
Chernyshev, V. V. & Schenk, H. (1998). *Z. Kristallogr.* **213**, 1–3.
Cohen-Addad, C., Lehmann, M. S., Becker, P., Parkanyi, L. & Kalman, A. (1984). *J. Chem. Soc. Perkin Trans.* 2, pp. 191–196.
Dewar, M. J. S., Zoebisch, E. G., Healy, E. F. & Stewart, J. J. P. (1985). *J. Am. Chem. Soc.* **107**, 3902–3909.
Dollase, W. A. (1986). *J. Appl. Cryst.* **19**, 267–272.
Gallay, J. J. & Schweizer, E. (1980). Eur. Patent 0041046.
Itoh, K. & Okonogi, K. (1995). US Patent 5387599.
Laikov, D. N. (1997). *Chem. Phys. Lett.* **281**, 151–156.
Lee, C., Yang, W. & Parr, R. G. (1988). *Phys. Rev. B*, **37**, 785–789.
Lerchen, H.-G., Von Dem Bruch, K., Petersen, U., Gaumgarten, J., Piel, N., Antonicek, H.-P., Weichel, W., Sperzel, M. & Bremm, K. D. (1996). WO Patent 9631532.
Low, J. N., Storey, E. J., McCarron, M., Wardell, J. L., Ferguson, G. & Glidewell, C. (2000). *Acta Cryst.* B**56**, 58–67.
Makarov, V. A., Ryabova, O. B., Chernyshev, V. V., Sonneveld, E. J. & Granik, V. G. (2001). *Chem. Heterocycl. Compd.* In the press.
Makarov, V. A., Sedov, A. L., Nemeryuk, M. P., Solovyeva, N. P., Anisimova, O. S. & Safonova, T. S. (1994). *Chem. Heterocycl. Compd*, pp. 1420–1423.
Nardelli, M. (1983). *Comput. Chem.* **7**, 95–98.
Philips (1996). *PROFIT for Windows*. Release 1.0*b*. Philips Analytical X-ray BV, Almelo, The Netherlands.
Rasheed, K. & Warkentin, J. D. (1977). *J. Org. Chem.* **42**, 1265.
Sheldrick, G. M. (1993). *SHELXL*93. University of Göttingen, Germany.
Spek, A. L. (1992). *PLUTON*92. University of Utrecht, The Netherlands.
Stewart, J. J. P. (1990). *MOPAC*6.0. QCPE Program No. 455. Quantum Chemistry Program Exchange, Department of Chemistry, Indiana University, Bloomington, Indiana, USA.
Storer, J. W., Giesen, D. J., Cramer, C. J. & Truhlar, D. G. (1995). *J. Comput. Aided Mol. Des.* **9**, 87–110.
Tokuhisa, K., Katsuura, K., Goda, M., Inoue, Y., Itoh, H., Ishida, N., Yamamoto, T., Yamauchi, K., Tokunaga, T. & Matsuno, S. (1998). WO Patent 9830539.
Visser, J. W. (1969). *J. Appl. Cryst.* **2**, 89–95.
Visser, J. W. (1986). *Powder Diffract.* **1**, 66–76.
Zlokazov, V. B. & Chernyshev, V. V. (1992). *J. Appl. Cryst.* **25**, 447–451.